

# Statistics of work performed by optical tweezers with general time-variation of their stiffness

Petr Chvosta<sup>1</sup>, Dominik Lips<sup>2</sup>, Viktor Holubec<sup>1,3</sup>,  
Artem Ryabov<sup>1</sup>, and Philipp Maass<sup>2</sup>

<sup>1</sup> Charles University, Faculty of Mathematics and Physics, Department of Macromolecular Physics, V Holešovičkách 2, CZ-180 00 Praha, Czech Republic

<sup>2</sup> Universität Leipzig, Institut für Theoretische Physik, Postfach 100 920, D-04009 Leipzig, Germany

<sup>3</sup> Universität Osnabrück, Fachbereich Physik, Barbarastrasse 7, 49076 Osnabrück, Germany

E-mail: Petr.Chvosta@mff.cuni.cz, dlips@uos.de, viktor.holubec@gmail.com, maass@uos.de, rjabov.a@gmail.com

March 2020

**Abstract.** We derive an exact expression for the probability density of work done on a particle that diffuses in a parabolic potential with a stiffness varying by an arbitrary piecewise constant protocol. Based on this result, the work distribution for time-continuous protocols of the stiffness can be determined up to any degree of accuracy. This is achieved by replacing the continuous driving by a piecewise constant one with a number  $n$  of positive or negative steps of increasing or decreasing stiffness. With increasing  $n$ , the work distributions for the piecewise protocols approach that for the continuous protocol. The moment generating function of the work is given by the inverse square root of a polynomial of degree  $n$ , whose coefficients are efficiently calculated from a recurrence relation. The roots of the polynomials are real and positive (negative) steps of the protocol are associated with negative (positive) roots. Using these properties the inverse Laplace transform of the moment generating function is carried out explicitly. Fluctuation theorems are used to derive further properties of the polynomials and their roots.

*Keywords:* Work statistics, fluctuation theorems, parabolic potential, nonequilibrium dynamics, Brownian motion

Submitted to: *J. Phys. A: Math. Gen.*

## 1. Introduction

Work, heat and entropy, when defined microscopically for individual trajectories have attracted much attention in nonequilibrium statistical physics [1–4], and form key quantities in stochastic thermodynamics [5]. Probability distributions of work fulfil detailed and integral fluctuation theorems [6–13]. These apply to nonequilibrium systems that are externally driven by a time-dependent protocol of control variables. The theorems hold true universally and allow one to determine free energy differences between equilibrium states from nonequilibrium processes. They represent refinements of the second law of thermodynamics and can be applied to extract equilibrium information from nonequilibrium measurements [14–22] either by using the Crooks theorem [23, 24] or the Jarzynski identity [25, 26]. For the Crooks theorem one needs to compare work distributions for a time-forward and a time-reversed process [27], which is not always possible in practice. A direct application of the Jarzynski identity would require to extend measured work probability distributions to large negative values. For this reason, it is important to have analytical expressions for work distributions for most common situations [28, 29].

Since forces applied in single-molecule experiments are often linear with respect to particle displacements, as, for example, those exerted by optical tweezers [30–35], the consideration of Brownian motion in time-varying harmonic potentials is particularly relevant. For the variation in time, two kinds of operation can be distinguished: in the first the minimum of the harmonic potential is changed with time (“moving parabola”) and in the second the stiffness of the potential is varied (“breathing parabola”). Analytical results for the work distribution could be derived for specific protocols in both modes of operation. Moreover, theories were developed to predict the exact asymptotic behaviour of work distributions [29, 36–40]. For the moving parabola with a potential minimum changing with time, the work distribution was calculated in Refs. [37, 41–45]. For general protocols of the breathing parabola, the problem can be reduced to the task of solving the Riccati equation [39], or, equivalently, of solving a system of coupled ordinary differential equations [46–48]. Explicit analytic results could be obtained for specific protocols only: (i) for a single sudden change [47], (ii) for slow driving, where the work distribution is Gaussian [46, 49], and (iii) and for a particular rational stiffness function [39, 48]. An Onsager-Machlup type of theory has been developed to obtain approximate solutions [50].

In the breathing parabola problem, the derivation of analytical solutions for work distributions seems to be impossible for general protocols. Here we derive an explicit solution for the joint probability of work and particle position, which is exact for protocols consisting of a sequence of instantaneous changes (steps) of the stiffness. Among others, this solution can be used to determine work distributions for time-continuous protocols with arbitrary accuracy by systematically increasing the number of steps in a discretization of the respective protocol. In contrast to general algorithms based on a numerical solution of the Fokker-Planck equation [51], the present

methodology significantly reduces computational costs and provides valuable analytical insights.

The paper is structured as follows. In Sec. 2 we outline the general method to obtain work distributions based on a few key equations, and demonstrate its power for a representative example. In Sec. 3 we present the methodology of our approach. The main results are explicit formulas for the joint probability of work and particle position [Eqs. (44) and (43)], and for the moment generating function of the work [Eqs. (48) and (47)] in terms of a polynomial  $Q_n$ . In Sec. 4 we derive recurrence relations for the  $Q_n$ , discuss properties of the roots of the polynomial and perform the inverse Laplace transform of the moment generating function. Section 5 summarizes our main findings and discusses their broader relevance, including perspectives for future work.

## 2. Method and representative examples

We consider the overdamped Brownian motion of a single particle in an external harmonic potential

$$V(x, t) = \frac{1}{2}k(t)x^2, \quad (1)$$

with time-varying stiffness  $k(t)$ . The stochastic process of the particle position is denoted by  $X(t)$  and evolves in time according to the Langevin equation

$$\frac{dX(t)}{dt} = -\mu k(t)X(t) + \sqrt{2D}\zeta(t), \quad (2)$$

where  $D$  is the diffusion constant,  $\mu = \beta D$  the mobility, and  $\beta = 1/(k_B T)$ , with  $k_B$  the Boltzmann constant and  $T$  the temperature;  $\zeta(t)$  is a Gaussian white noise with zero mean and correlator  $\langle \zeta(t)\zeta(t') \rangle = \delta(t - t')$ .

Each stochastic trajectory in a time interval  $[0, t]$  yields a value of the work done on the particle, i.e. the work process  $W(t)$  is a functional of the Markov process  $X(t')$ ,  $0 \leq t' \leq t$ ,

$$W(t) = \int_0^t dt' \frac{\partial V(X(t'), t')}{\partial t'} = \frac{1}{2} \int_0^t dt' \dot{k}(t') X^2(t'). \quad (3)$$

The work by itself is not a Markov process. However, the combined process  $(X(t), W(t))$  is still a time-nonhomogeneous Markov process and its joint probability density  $\Phi_{X,W}(x, w, t)$  obeys a Fokker-Planck equation [see Eq. (37) below].

Let  $k(t)$  be a piecewise constant protocol exhibiting  $n$  steps in the time interval  $[0, t]$  at time instants  $t_1, \dots, t_n$  with  $0 \equiv t_0 < t_1 < t_2 < \dots < t_n < t$ ,  $k(t) = k_j$  in each time segment  $[t_j, t_{j+1}[$ , and starting value  $k(0) = k_0 > 0$ . In terms of the scaled stiffnesses (relaxation rates)  $\gamma_j = \mu k_j$ ,  $j = 0, \dots, n$ , this protocol can be written as

$$\gamma(t) = \gamma_0 + \sum_{j=1}^n (\gamma_j - \gamma_{j-1}) \Theta(t - t_j), \quad (4)$$

where  $\Theta(\cdot)$  is the Heaviside step function [ $\Theta(x) = 1$  for  $x \geq 0$  and zero otherwise].

We are interested in the work distribution  $\Phi_n(w)$  for the protocol  $\gamma_n(t)$  and an initial state, where the particle is equilibrated in the potential  $V(x, 0)$ . As shown in Sec. 3, starting from the Fokker-Planck equation for  $\Phi_{\mathbf{x}, \mathbf{w}}(x, w, t)$  and utilizing properties of the propagator for the position process, one can derive an exact analytical result for the bilateral Laplace transform  $\tilde{\Phi}_n(u)$  of  $\Phi_n(w)$ . The result is

$$\tilde{\Phi}_n(u) = \int_{-\infty}^{+\infty} dw e^{-uw} \Phi_n(w) = \frac{1}{\sqrt{Q_n(u/\beta)}} \quad (5)$$

with

$$Q_n(\xi) = \sum_{j=0}^n q_j \xi^j \quad (6)$$

a polynomial of degree  $n$ . Defining

$$\eta_j = \exp[-2\gamma_j(t_{j+1} - t_j)] , \quad (7)$$

$$\epsilon_j = \frac{\gamma_j - \gamma_{j-1}}{\gamma_0} \eta_{j-1} \eta_{j-2} \dots \eta_1 , \quad (8)$$

$$\phi_j = \frac{\gamma_0}{\gamma_j} \frac{1 - \eta_j}{\eta_j \eta_{j-1} \dots \eta_1} , \quad (9)$$

the polynomial  $Q_n(\xi)$  can be calculated from the recursion relation

$$Q_n(\xi) = Q_{n-1}(\xi) + \xi \epsilon_n \left[ 1 + \sum_{j=1}^{n-1} \phi_j Q_j(\xi) \right] . \quad (10)$$

The initial condition is  $Q_0(\xi) = 1$  as without a step, no work is done and accordingly  $\Phi_0(w, t) = \delta(w)$  and  $\tilde{\Phi}_n(u) = 1$ . An explicit expression for the coefficients  $q_j$  in Eq. (6) is derived in Sec. 4.2 and reads

$$q_j = \sum_{i_1=1}^{n-j+1} \epsilon_{i_1} \phi_{i_1-1,0} \sum_{i_2=i_1+1}^{n-j+2} \epsilon_{i_2} \phi_{i_2-1,i_1} \dots \sum_{i_j=i_{j-1}+1}^n \epsilon_{i_j} \phi_{i_j-1,i_{j-1}} , \quad (11)$$

where

$$\phi_{j_2, j_1} = \sum_{j=j_1}^{j_2} \phi_j . \quad (12)$$

Expanding both sides of Eq. (5) into a power series in the variable  $u$ , we see that the coefficients  $q_j$  determine the moments of the work  $\mathbf{W}_n$  after  $n$  steps. For example, the mean work is given by  $\beta \langle \mathbf{W}_n \rangle = q_1/2$  and the second moment by  $\beta^2 \langle \mathbf{W}_n^2 \rangle = -q_2 + 3q_1^2/4$ .

To invert the bilateral Laplace transform in Eq. (5), the polynomial  $Q_n(\xi)$  is factored into its roots. All roots are distinct and located on the real axis. The roots are connected with the protocol steps: each positive step [increase of stiffness,  $(\gamma_{j+1} - \gamma_j) > 0$ ] gives a negative root and each negative step [decrease of stiffness,  $(\gamma_{j+1} - \gamma_j) < 0$ ] gives a positive root. Hence the  $n_-$  negative roots  $\xi_j^- < 0$  and  $n_+$  positive roots  $\xi_j^+ > 0$  contribute to  $\Phi_n(w)$  at positive and negative  $w$ , respectively. We order the  $n_{\pm}$  roots according to their magnitude:

$$0 < |\xi_1^-| < |\xi_2^-| < \dots < |\xi_{n_-}^-| < \infty , \quad (13)$$

$$0 < \xi_1^+ < \xi_2^+ < \dots < \xi_{n_+}^+ < \infty . \quad (14)$$

Writing

$$Q_n(\xi) = q_n \prod_{j=1}^{n_-} (\xi - \xi_j^-) \prod_{k=1}^{n_+} (\xi - \xi_k^+), \quad (15)$$

the inverse Laplace transform of  $\tilde{\Phi}_n(u)$  in Eq. (5) gives

$$\Phi_n(w) = \frac{\beta}{\sqrt{q_n}} \int_{-i\infty}^{+i\infty} \frac{d\xi}{2\pi i} \frac{\exp(\beta w \xi)}{\sqrt{\prod_{j=1}^{n_-} (\xi - \xi_j^-) \prod_{k=1}^{n_+} (\xi - \xi_k^+)}}. \quad (16)$$

This integral can be calculated by a contour integration along closed paths encircling the negative and positive real axes, where branch cuts between neighbouring pairs of roots give definite integral contributions. The details are described in Sec. 4.3 and the final result is:

$$\Phi_n(w) = \Phi_n^-(w)\Theta(-w) + \Phi_n^+(w)\Theta(w), \quad (17)$$

$$\Phi_n^+(w) = \beta \sum_{j=1}^{m_-} (-1)^j I_n(\beta w; \xi_{2j}^-, \xi_{2j-1}^-) + \beta \begin{cases} 0, & n_- \text{ even} \\ (-1)^{1+m_-} I_n(\beta w; -\infty, \xi_{n_-}^-), & n_- \text{ odd} \end{cases} \quad (18)$$

$$\Phi_n^-(w) = \beta \sum_{j=1}^{m_+} (-1)^j I_n(\beta w; \xi_{2j}^+, \xi_{2j-1}^+) + \beta \begin{cases} 0, & n_+ \text{ even} \\ (-1)^{1+m_+} I_n(\beta w; \xi_{n_+}^+, \infty), & n_+ \text{ odd} \end{cases} \quad (19)$$

where

$$m_{\pm} = \begin{cases} \frac{n_{\pm}}{2}, & n_{\pm} \text{ even} \\ \frac{n_{\pm} - 1}{2}, & n_{\pm} \text{ odd} \end{cases} \quad (20)$$

and

$$I_n(\theta; a, b) = C_n \int_a^b \frac{dx}{\pi} \frac{\exp(\theta x)}{\sqrt{\prod_{j=1}^{n_-} |\xi - \xi_j^-| \prod_{k=1}^{n_+} |\xi - \xi_k^+|}} \quad (21)$$

with

$$C_n = -\frac{1}{i^{n_+} \sqrt{q_n}} = \frac{1}{\sqrt{\prod_{j=1}^{n_-} |\xi_j^-| \prod_{k=1}^{n_+} \xi_k^+}}. \quad (22)$$

This means that to calculate  $\Phi_n(w)$ , one needs to find the roots  $\xi_j^{\pm}$  and to evaluate the integrals  $I_n(\beta w; \xi_{2j}^{(\pm)}, \xi_{2j+1}^{(\pm)})$  from Eq. (21).

Figure 1 illustrates the work probability density function (PDF) for several protocols with a small number of steps. In all left panels [(a), (c), and (e)] the stiffness increases with time (no negative steps in the protocol). Accordingly, the work assumes positive values only. With increasing number of steps, the probability weight of small work values, corresponding to trajectories  $\mathbf{X}(t)$  dwelling close to the origin during all steps, decreases as can be seen from the different behaviours of  $\Phi_1$ ,  $\Phi_2$ ,  $\Phi_3$  around  $w = 0$ . This can be also understood from the limit  $\Phi_n(0^+) = \lim_{u \rightarrow \infty} u \tilde{\Phi}_n(u)$ . For one step [panel (a)], we have only one root, hence the limit diverges. For two steps, there

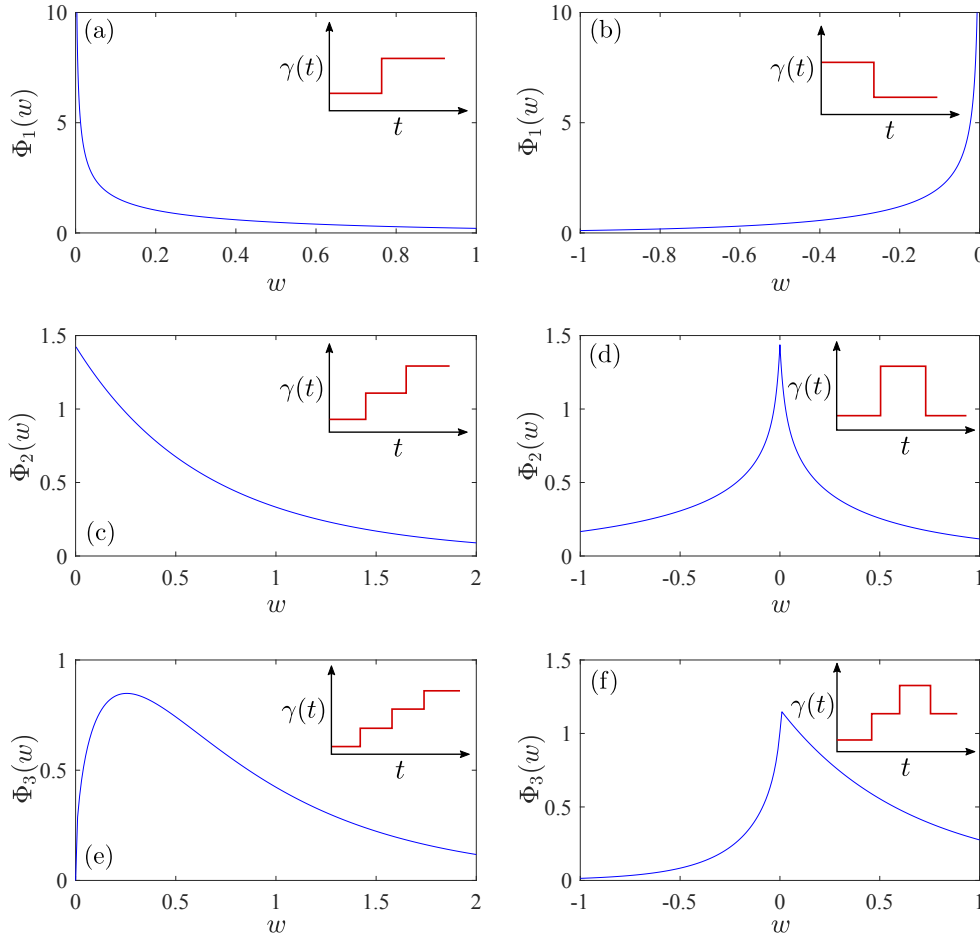


**Figure 1.** Work PDFs  $\Phi_n(w)$  for protocols with  $n = 1, 2$ , and  $3$  steps, which are illustrated in the respective insets. In all panels except (b), the starting value of the protocol is  $\gamma_0 = 1$ . The duration of all protocol segments is  $1$ . The step size is always equal to  $1$ . In the panel (b), the time-reversed protocol of the case (a) is considered. Work is given in units of  $k_B T$ , work PDFs in units of  $\beta = 1/(k_B T)$ , and time in units of  $1/\gamma_0$ .

are two roots and the limit is finite [panel (c)]. For three and more steps, the limit is zero.

The right column of Fig. 1 [panels (b), (d), and (e)] shows examples of work PDFs for protocols that have one negative step. Accordingly, the work can assume negative values also. The probability weight of the positive work values increases with the number of positive steps. The work PDF is always continuous at  $w = 0$  whenever both negative and positive steps are present in the protocol.

To demonstrate how well a work distribution for a continuous protocol can be approximated by that of a piecewise constant protocol, we consider  $\gamma(t) = \gamma_0[2 + \sin(\omega t)]$  with  $\gamma_0/\omega = 1$  in the time interval  $[0, t_f]$ ,  $t_f = \pi/\omega$ . This corresponds to “one sinusoidal breath of the parabola”. For constructing the piecewise constant protocols, we use equidistant time steps, i.e.  $t_j = jt_f/(n + 1)$ ,  $j = 0, 1, \dots, n + 1$  and  $\gamma_j = \gamma(t_j)$ . The

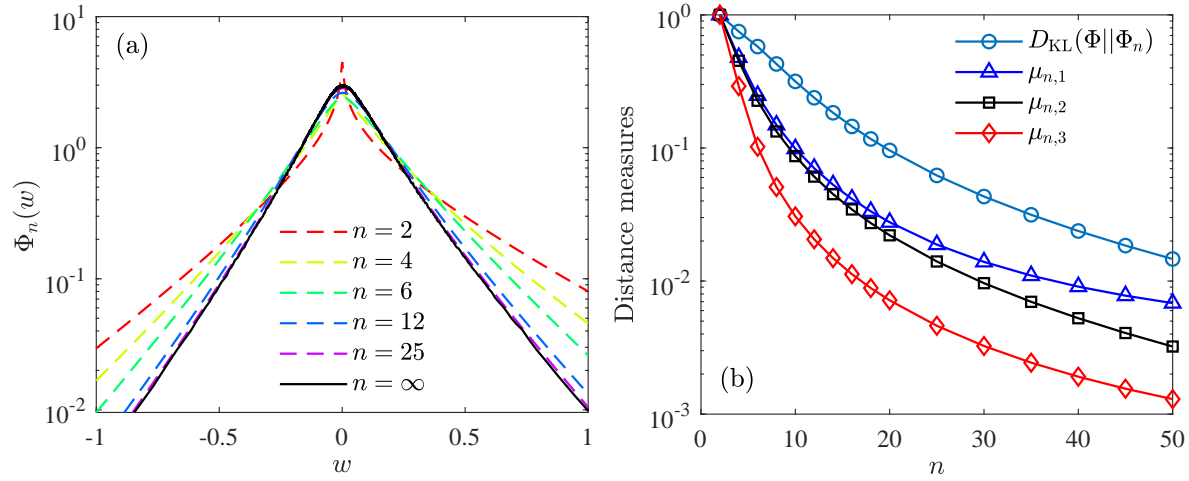


**Figure 2.** (a) Simulated work distribution  $\Phi(w)$  (solid line, denoted as  $n = \infty$ ) for the continuous protocol  $\gamma(t) = \gamma_0[2 + \sin(\omega t)]$  with  $\gamma_0/\omega = 1$  in comparison with distributions  $\Phi_n(w)$  for the piecewise constant protocols. (b) Kullback-Leibler divergences  $D_{\text{KL}}(\Phi||\Phi_n)$  of the  $\Phi_n(w)$  approximations of  $\Phi(w)$  and scaled relative deviations  $\mu_{n,k}$  of the  $k$ -th moments in the  $n$ -th step approximations as functions of  $n$ .

corresponding work distribution  $\Phi_n(w)$  is obtained as described above: we first calculate the polynomial  $Q_n(\xi)$  in Eq. (6) by using the recurrence relation Eq. (10), then determine its roots  $\xi_j^\pm$ , and finally evaluate Eqs. (18) and (19) with the integrals given in Eq. (21).

The work distribution  $\Phi(w)$  for the continuous protocol was determined by Brownian dynamics simulations based on  $10^7$  realizations of the process. Figure 2(a) shows how the  $\Phi_n(w)$  (dashed lines) approach the  $\Phi(w)$  (solid line) with increasing  $n$ . For just  $n = 12$  steps we already obtain a good approximation for  $\Phi(w)$ , and for  $n = 25$  the  $\Phi_n(w)$  can hardly be distinguished from  $\Phi(w)$  (for the scales of the axes used in the figure).

To quantify the goodness of the approximation, we introduce the following distance measures: the Kullback-Leibler divergence  $D_{\text{KL}}(\Phi||\Phi_n) = \int dw \Phi(w) \ln[\Phi(w)/\Phi_n(w)]$ , and the relative deviations  $\Delta_{n,k} = |\langle W^k \rangle_{\Phi_n} - \langle W^k \rangle_\Phi| / \langle W^k \rangle_\Phi$  of the  $k$ th moments in the  $n$ th step approximation. The results are shown in Fig. 2(b) in a semi-logarithmic representation. To include the  $\Delta_{n,k}$  in the same plot as the  $D_{\text{KL}}(\Phi||\Phi_n)$ , we scaled the corresponding values with respect to  $\Delta_{2,k}$ , i.e. we plotted  $\mu_{n,k} = \Delta_{n,k}/\Delta_{2,k}$ . With increasing  $n$ , both the  $D_{\text{KL}}(\Phi||\Phi_n)$  and the  $\mu_{n,k}$  rapidly decrease to zero.

Let us note that it is not required to take equidistant time steps. The time discretization can be adapted specifically to a given protocol. For example, the convergence with increasing number of steps should improve by requiring the changes of the stiffness in each step to be equal.

### 3. Analytical treatment in the Laplace domain

#### 3.1. Propagator for particle position

The particle position  $\mathbf{X}(t)$  follows a time-nonhomogeneous Markov process and its PDF  $\Phi_{\mathbf{X}}(x, t)$  satisfies the Fokker-Planck equation

$$\frac{\partial}{\partial t} \Phi_{\mathbf{X}}(x, t) = \left\{ D \frac{\partial^2}{\partial x^2} + \mu \frac{\partial}{\partial x} \left[ \frac{\partial}{\partial x} V(x, t) \right] \right\} \Phi_{\mathbf{X}}(x, t). \quad (23)$$

For the parabolic potential (1) with constant stiffness, its solution is a simple Gaussian PDF, and for the piecewise constant protocol with  $n$  jumps, the convolution of all Gaussian PDFs for the individual segments yields again a Gaussian PDF. Here we introduce an operator notation and rescaled variances of resulting PDFs, which will be used in the derivation of the work distribution.

For an arbitrary protocol  $\gamma(t)$ , the Green function of Eq. (23) is

$$G(x, t | x', t') = \frac{1}{\sqrt{2\pi v(t, t')}} \exp \left\{ -\frac{[x - m(t, t')x']^2}{2v(t, t')} \right\}, \quad (24)$$

where

$$m(t, t') = \exp \left[ -\int_{t'}^t ds \gamma(s) \right], \quad (25)$$

$$v(t, t') = 2D \int_{t'}^t ds \exp \left[ -2 \int_s^t ds' \gamma(s') \right]. \quad (26)$$

The Green function gives the solution of the Fokker-Planck equation for the initial condition  $\delta(x - x')$  at time  $t'$ . Notice that the time variables  $t, t'$  enter solely through the functions  $m(t, t')$  and  $v(t, t')$ . This motivates to consider the Green function as a matrix element of an operator  $\mathcal{G}(m, v)$  in the space of continuous functions of  $x$ :

$$\langle x | \mathcal{G}(a, b) | x' \rangle = \frac{1}{\sqrt{2\pi b}} \exp \left[ -\frac{(x - ax')^2}{2b} \right] \quad (27)$$

for  $a, b > 0$  real. This operator satisfies the composition rule

$$\mathcal{G}(a_2, b_2) \mathcal{G}(a_1, b_1) = \mathcal{G}(a_2 a_1, b_2 + a_2^2 b_1). \quad (28)$$

Similarly, if the operator  $\mathcal{G}(a, b)$  acts on a state  $|\mathbf{g}(c)\rangle$  that in position representation is a Gaussian PDF with zero mean and variance  $c$ , one obtains

$$\mathcal{G}(a, b) |\mathbf{g}(c)\rangle = |\mathbf{g}(b + a^2 c)\rangle. \quad (29)$$

Let us now consider the piecewise constant protocol in Eq. (4). Using the Markov property, the Green function  $\mathcal{G}_n(t)$  for the interval  $(0, t)$  is a product of the propagators for the individual segments,

$$\mathcal{G}_n(t) = \mathcal{G}(m(t, t_n), v(t, t_n)) \mathcal{G}(m_{n-1}, v_{n-1}) \dots \mathcal{G}(m_1, v_1) \mathcal{G}(m_0, v_0), \quad (30)$$

where  $m_j = \eta_j^{1/2}$  and  $v_j = (D/\gamma_j)(1 - \eta_j)$  with  $\eta_j$  given in Eq. (7). For the following, it is convenient to define the segment parameters

$$\psi_j = \frac{\gamma_0}{D} v_j = \frac{\gamma_0}{\gamma_j} (1 - \eta_j) \quad (31)$$



that depend on the duration of the segments and on the respective values of the protocol. Notice that for any signs of the protocol parameters  $\gamma_j$  the  $\psi_j$  are always positive. If the duration of the segment following the  $j$ -th step is zero, its parameters are  $\eta_j = 1$ ,  $\psi_j = 0$ . If the length tends to infinity and if  $\gamma_j > 0$ , we have  $\eta_j \rightarrow 0$ , and  $\psi_j \rightarrow \gamma_0/\gamma_j$ . For negative  $\gamma_j$ ,  $\eta_j \rightarrow \infty$ , and  $\psi_j \rightarrow \infty$ .

The initial PDF  $\Phi_{\mathbf{X}}(x, 0)$  is considered to describe a particle equilibrated in the potential  $V(x, 0)$ , i.e.  $\Phi_{\mathbf{X}}(x, 0) \propto \exp[-\beta V(x, 0)]$  (assuming  $k_0 > 0$ ). The initial state remains unchanged during the zeroth segment. After the first step of the protocol, the variance either decreases (for  $\gamma_1 > \gamma_0$ ), or increases (for  $\gamma_1 < \gamma_0$ ). The state at the final time  $t$  is  $\mathcal{G}_n(t)|\mathbf{g}(v_0)\rangle$ .

We now use Eq. (29) to relate variances  $v(t, 0)$  [see Eq. (26)] at consecutive times  $t_j$  and  $t_{j+1}$ ,

$$v(t_{j+1}, 0) = v_0\psi_j + \eta_j v(t_j, 0), \quad j = 1, \dots, n-1, \quad (32)$$

where  $v_0 = v(t_1, 0) = v(0, 0)$ . For the following it is convenient to introduce the scaled variances

$$r_j = \frac{v(t_{j+1}, 0)}{v_0 \eta_j \eta_{j-1} \dots \eta_1}, \quad j = 1, \dots, n-1, \quad (33)$$

and  $r_0 = 1$ . Inserting these into Eq. (32) yields the recursion relation

$$r_j = \phi_j + r_{j-1} \quad (34)$$

with

$$\phi_j = \frac{\psi_j}{\eta_j \eta_{j-1} \dots \eta_1}. \quad (35)$$

After inserting  $\psi_j$  from Eq. (31) this gives Eq. (9). The solution of the recursion relation (34) is

$$r_j = \phi_j + \phi_{j-1} + \dots + \phi_1 + 1. \quad (36)$$

### 3.2. Propagator for the composed process

The work done on the particle depends on the whole particle trajectory, i.e. the work process  $\mathbf{W}(t)$  is a functional of the position process  $\mathbf{X}(t)$ . The work by itself is not a Markov process. However, the combined process  $(\mathbf{X}(t), \mathbf{W}(t))$  is a time-nonhomogeneous Markov process and its joint PDF follows from the equation [52, 53]

$$\frac{\partial}{\partial t} \Phi_{\mathbf{X}, \mathbf{W}}(x, w, t) = \left\{ D \frac{\partial^2}{\partial x^2} + \mu \frac{\partial}{\partial x} \left[ \frac{\partial}{\partial x} V(x, t) \right] - \left[ \frac{\partial}{\partial t} V(x, t) \right] \frac{\partial}{\partial w} \right\} \Phi_{\mathbf{X}, \mathbf{W}}(x, w, t). \quad (37)$$

The first two operators on the right-hand side (RHS) are the same as in the Fokker-Planck equation (23) and reflect the possibility that the combined process leaves the two-dimensional interval  $[x, x + dx] \times [w, w + dw]$  because of a change of the particle position. The third operator on the RHS describes the time change of the probabilistic weight of this interval caused by the work done on the particle with its position fixed.

At the initial time there has been no work done yet. Therefore the initial condition is  $\Phi_{\mathbf{x},\mathbf{w}}(x, w, 0) = \langle x | \mathbf{g}(v_0) \rangle \delta(w)$ .

The full information given by the joint PDF can be extracted from its double-sided Laplace transformation with respect to the work variable  $w$ . We designate the transformed joint PDF as  $\tilde{\Phi}_{\mathbf{x},\mathbf{w}}(x, u, t)$ , where  $u$  is the complex variable conjugated to  $w$ . After the transformation, the partial derivative over  $w$  becomes a multiplication by  $u$ . We thus obtain

$$\frac{\partial}{\partial t} \tilde{\Phi}_{\mathbf{x},\mathbf{w}}(x, u, t) = \left\{ D \frac{\partial^2}{\partial x^2} + \gamma(t) \frac{\partial}{\partial x} x + \frac{1}{2} \frac{\dot{\gamma}(t)}{D} x^2 \frac{u}{\beta} \right\} \tilde{\Phi}_{\mathbf{x},\mathbf{w}}(x, u, t), \quad (38)$$

where  $\dot{\gamma}(t)$  is the time derivative of the protocol function  $\gamma(t)$ .

The task of solving the dynamical equation (38) requires the calculation of a time-ordered exponential operator. This is known to be a hard mathematical problem. However, for the piecewise constant protocol, the time derivative  $\dot{\gamma}(t)$  in Eq. (38) is a sum of delta functions. Hence the time integrals in the underlying Dyson series can be carried out. The details of this step, in a quite different context, are explained in [54]. We now pursue this key idea.

We insert into Eq. (38)  $\gamma(t)$  from Eq. (4) and treat the third term on the RHS as a time-dependent perturbation with respect to the evolution controlled by the first two terms. Using the operator notation, we designate the Green function corresponding to Eq. (38) and to the protocol (4) as  $\tilde{\mathcal{G}}_n(u, t)$ ,  $t \geq t_n$ . It is again an operator acting in the space of  $x$ -functions. After removing the multiple integrals from the Dyson series, we find

$$\begin{aligned} \tilde{\mathcal{G}}_n(u, t) &= \mathcal{G}(m(t, t_n), v(t, t_n)) \exp \left( -\frac{\gamma_n - \gamma_{n-1}}{2D} \xi \mathcal{X}^2 \right) \\ &\quad \times \mathcal{G}(m_{n-1}, v_{n-1}) \exp \left( -\frac{\gamma_{n-1} - \gamma_{n-2}}{2D} \xi \mathcal{X}^2 \right) \\ &\quad \vdots \\ &\quad \times \mathcal{G}(m_1, v_1) \exp \left( -\frac{\gamma_1 - \gamma_0}{2D} \xi \mathcal{X}^2 \right) \mathcal{G}(m_0, v_0), \end{aligned} \quad (39)$$

where

$$\xi = \frac{u}{\beta} \quad (40)$$

and  $\mathcal{X}$  is the position operator with matrix elements  $\langle x | \mathcal{X} | x' \rangle = x \delta(x - x')$ . Let us now derive a simple closed form expression for this Green function.

Consider the action of the operator  $\tilde{\mathcal{G}}_n(u, t)$  on the initial state  $|\mathbf{g}(v_0)\rangle$ . The rightmost operator  $\mathcal{G}(m_0, v_0)$  does not alter  $|\mathbf{g}(v_0)\rangle$ , i.e.,  $\mathcal{G}(m_0, v_0) |\mathbf{g}(v_0)\rangle = |\mathbf{g}(v_0)\rangle$ . Applying the two further rightmost operators yields

$$\mathcal{G}(m_1, v_1) \exp \left( -\frac{\gamma_1 - \gamma_0}{2D} \xi \mathcal{X}^2 \right) |\mathbf{g}(v_0)\rangle = \frac{1}{\sqrt{1 + \xi(\gamma_1 - \gamma_0)/\gamma_0}} |\mathbf{g}(v_0 \eta_1 R_1(\xi))\rangle, \quad (41)$$

where  $R_1(\xi) = \phi_1 + 1/[\xi(\gamma_1 - \gamma_0)/\gamma_0 + 1]$  and the expression on the RHS can be viewed as a non-normalized Gaussian PDF with a  $\xi$ -dependent complex variance.

Repeating the procedure, there emerges a regular pattern, which allows one to write  $\tilde{\mathcal{G}}_n(u, t)$  in a compact form. This comprises a sequence of rational functions  $R_j(\xi)$ ,  $j = 0, \dots, (n-1)$ , that are generated by the recurrence relation

$$R_j(\xi) = \phi_j + \frac{1}{\xi\epsilon_j + \frac{1}{R_{j-1}(\xi)}}, \quad (42)$$

with  $R_0(\xi) = 1$  and  $\epsilon_j$  given in Eq. (8). An important property of the recurrence equation (42) is that it coincides with Eq. (34) for  $\xi = 0$ . Hence,  $R_j(0) = r_j$  is the scaled variance at the end of the  $j$ -th segment. For an arbitrary  $\xi$ , the explicit solution of Eq. (42) is a finite regular continued fraction

$$R_j(\xi) = \phi_j + \frac{1}{\xi\epsilon_j + \frac{1}{\phi_{j-1} + \frac{1}{\xi\epsilon_{j-1} + \frac{1}{\ddots \phi_1 + \frac{1}{\xi\epsilon_1 + 1}}}}}. \quad (43)$$

The final expression for the Green function is

$$\tilde{\mathcal{G}}_n(u, t) | \mathbf{g}(v_0) \rangle = \frac{1}{\sqrt{\prod_{j=1}^n [1 + \xi\epsilon_j R_{j-1}(\xi)]}} \left| \mathbf{g} \left( v(t, t_n) + v_0 m^2(t, t_n) \frac{R_{n-1}(\xi) \eta_{n-1} \eta_{n-2} \dots \eta_1}{1 + \xi\epsilon_n R_{n-1}(\xi)} \right) \right\rangle. \quad (44)$$

This result gives the full information on the statistics of work and position. It allows one to calculate also correlations between any functions of these random variables. In particular, it can be applied to generalized periodic protocols and initial conditions, which resemble periodic processes in pumps or motors on a molecular scale [55–61]. Some of these applications would require to extend the above findings to a time-dependent temperature, which is straightforward because it just leads to modified step parameters. A generalization of the presented methodology to other functionals of the particle position such as heat or dwelling times [51] should be also possible.

A more difficult problem is to extend the above method to a particle initially placed at a given point, corresponding to a  $\delta$ -function. This will introduce a nonzero mean value into the Gaussian states in Eq. (39) and significantly affect the recurrence relations. Mathematical structure of such generalizations can appear in various problems involving quadratic functionals of Gaussian processes, e.g., in the analysis of mean-squared displacements in single-particle tracking experiments [62, 63].

### 3.3. Moment generating function of work

For the Laplace transform of the work PDF  $\Phi_n(w)$ , the result (44) yields

$$\tilde{\Phi}_n(u) = \langle e^{-uW_n} \rangle = \int_{-\infty}^{\infty} dx \langle x | \tilde{\mathcal{G}}_n(u, t) | \mathbf{g}(v_0) \rangle = \frac{1}{\sqrt{\prod_{j=1}^n [1 + \xi \epsilon_j R_{j-1}(\xi)]}}, \quad (45)$$

where  $\xi = u/\beta$  [see Eq. (40)] and the final time  $t > t_n$  is irrelevant, because during the interval  $(t_n, t)$  the protocol assumes the constant value  $\gamma_n$  and hence no work is done.

Equation (45) is the second important result. However, the  $u$ - (or  $\xi$ -)dependence of the result seems to be quite involved. For example, it is unclear how one could calculate the derivatives of the function  $\tilde{\Phi}_n(u)$ . These derivatives, evaluated at  $u = 0$ , are needed to get the moments  $\langle W_n^k \rangle$ . Fortunately, the matter is simpler, because the finite product in (45) is a polynomial of degree  $n$  in the complex variable  $\xi$ , which we prove next.

We already know that the functions  $R_k(\xi)$  are given by the finite continued fractions in Eq. (43). These fractions can be represented as ratios of two polynomials,

$$R_k(\xi) = \frac{P_k(\xi)}{Q_k(\xi)}. \quad (46)$$

Upon inserting this form into the recurrence relations (42) one arrives at a system of two linear difference equations, which can be written in matrix form as

$$\begin{aligned} \begin{pmatrix} P_k(\xi) \\ Q_k(\xi) \end{pmatrix} &= \begin{pmatrix} \xi \epsilon_k \phi_k + 1 & \phi_k \\ \xi \epsilon_k & 1 \end{pmatrix} \begin{pmatrix} P_{k-1}(\xi) \\ Q_{k-1}(\xi) \end{pmatrix} = \begin{pmatrix} 1 & \phi_k \\ 0 & 1 \end{pmatrix} \begin{pmatrix} 1 & 0 \\ \xi \epsilon_k & 1 \end{pmatrix} \begin{pmatrix} P_{k-1}(\xi) \\ Q_{k-1}(\xi) \end{pmatrix} \\ &= \mathbb{R}(\phi_k) \mathbb{L}(\xi \epsilon_k) \begin{pmatrix} P_{k-1}(\xi) \\ Q_{k-1}(\xi) \end{pmatrix} \end{aligned} \quad (47)$$

with  $P_0(\xi) = 1$  and  $Q_0(\xi) = 1$ . In the last expression we introduced the one-parameter families of the two-by-two matrices  $\mathbb{R}(\cdot)$  and  $\mathbb{L}(\cdot)$ . They are helpful for gaining deeper insight into the work PDF.

The finite product in Eq. (45) equals to the polynomial  $Q_n(\xi)$ , i.e.,

$$\tilde{\Phi}_n(u) = \frac{1}{\sqrt{Q_n(u/\beta)}}, \quad (48)$$

which can be readily proved by induction: for  $n = 1$  the assertion is obviously true. Suppose it is valid for  $n = k - 1$ . Then, using the second row in Eq. (47), it is also valid for  $n = k$ .

## 4. Probability density of work

The expressions of the polynomials  $Q_n(\xi)$  are made more explicit in the following two subsections 4.1 and 4.2. The work PDF is obtained in subsection 4.3 by factoring  $Q_n(\xi)$  into its roots and by performing the inverse Laplace transform of  $\tilde{\Phi}_n(u)$  via contour integration along closed paths encircling the negative and positive real axes.

#### 4.1. Solution of the recurrence equations

The recurrence equations (47) yield the formal solution

$$P_n(\xi) = \langle 1, 0 | \mathbb{R}(\phi_n) \mathbb{L}(\xi \epsilon_n) \mathbb{R}(\phi_{n-1}) \mathbb{L}(\xi \epsilon_{n-1}) \dots \mathbb{R}(\phi_1) \mathbb{L}(\xi \epsilon_1) | 1, 1 \rangle, \quad (49)$$

$$Q_n(\xi) = \langle 0, 1 | \mathbb{L}(\xi \epsilon_n) \mathbb{R}(\phi_{n-1}) \mathbb{L}(\xi \epsilon_{n-1}) \dots \mathbb{R}(\phi_1) \mathbb{L}(\xi \epsilon_1) | 1, 1 \rangle. \quad (50)$$

Here and in the following we use the bra-ket notation: for a two-row column vector with elements  $x_1, x_2$ , we have  $x_1 = \langle 1, 0 | x_1, x_2 \rangle$ , and  $x_2 = \langle 0, 1 | x_1, x_2 \rangle$ . Notice that  $\langle 0, 1 | \mathbb{R}(x) = \langle 0, 1 |$ , which has been used in Eq. (50). As a consequence of Eq. (50), the  $Q_n(\xi)$  and hence the PDF  $\Phi_n(w)$  depend solely on the parameters  $\phi_k, k = 1, \dots, n-1$ , and  $\epsilon_k, k = 1, \dots, n$ .

There exists a recurrence formula which facilitates the numerical calculation of the polynomials  $Q_n(\xi)$ . To derive it, we start again with the representation (50) and insert the identity operator ( $|0, 1\rangle\langle 0, 1| + |1, 0\rangle\langle 1, 0|$ ) just after the matrix  $\mathbb{R}(\phi_{n-1})$ . The result is the sum of two expressions, one of them being  $(1 + \xi \epsilon_n \phi_{n-1}) Q_{n-1}(\xi)$ . The other is proportional to  $\xi \epsilon_{n-1}$  and we continue with its evaluation. After  $(n-1)$  recursive steps, we obtain

$$Q_n(\xi) = Q_{n-1}(\xi) + \xi \epsilon_n [\phi_{n-1} Q_{n-1}(\xi) + \phi_{n-2} Q_{n-2}(\xi) + \dots + \phi_1 Q_1(\xi) + 1]. \quad (51)$$

In view of the following discussion, it is expedient to elaborate on the single-step and the two-steps protocol. We get

$$P_1(\xi) = \epsilon_1 \phi_1 \xi + \phi_1 + 1, \quad (52)$$

$$Q_1(\xi) = \epsilon_1 \xi + 1, \quad (53)$$

$$P_2(\xi) = \epsilon_2 \epsilon_1 \phi_2 \phi_1 \xi^2 + [\epsilon_2 \phi_2 (\phi_1 + 1) + \epsilon_1 (\phi_1 + \phi_2)] \xi + \phi_2 + \phi_1 + 1, \quad (54)$$

$$Q_2(\xi) = \epsilon_2 \epsilon_1 \phi_1 \xi^2 + [\epsilon_2 (\phi_1 + 1) + \epsilon_1] \xi + 1. \quad (55)$$

Essentially, the form of the resulting PDF  $\Phi_1(w)$  is given by the root  $\xi_1 = -1/\epsilon_1$  of  $Q_1(\xi)$ , where  $\epsilon_1 = (\gamma_1 - \gamma_0)/\gamma_0$  [see Eq. (8)]. If  $\gamma_1 > \gamma_0$  (positive step) the root is negative. Performing the inverse Laplace transform  $\tilde{\Phi}_1(u) \rightarrow \Phi_1(w)$ , we find the work PDF to vanish for negative  $w$ . If  $\gamma_1 < \gamma_0$  (negative step) the root is positive and the work PDF vanishes for positive  $w$ . If  $\gamma_1$  is negative (inverted parabolic potential), the root lies in the interval  $(0, 1)$ . The explicit result valid for any  $\gamma_1$  reads

$$\Phi_1(w) = \frac{\beta}{\sqrt{\pi \epsilon_1 \beta w}} \exp\left(-\frac{\beta w}{\epsilon_1}\right) [\Theta(\gamma_1 - \gamma_0) \Theta(w) + \Theta(\gamma_0 - \gamma_1) \Theta(-w)]. \quad (56)$$

Simple analytical inversion  $\tilde{\Phi}_n(u) \rightarrow \Phi_n(w)$  is also possible in the two-step protocol. In that case the product of the two roots of  $Q_2(\xi)$  has the same sign as the product  $\epsilon_1 \epsilon_2$ . If both steps are positive (negative),  $\Phi_2(w)$  is nonzero for positive (negative)  $w$ . If the steps differ in sign, the work PDF is nonzero for all  $w$ . For example, for two positive steps yielding roots  $-\infty < \xi_1 < \xi_2 < 0$ , we obtain

$$\Phi_2(w) = \beta \sqrt{\xi_1 \xi_2} \text{I}_0\left(\frac{\beta w}{2}(\xi_2 - \xi_1)\right) \exp\left[\frac{\beta w}{2}(\xi_2 + \xi_1)\right] \Theta(w), \quad (57)$$

where  $I_0(x)$  is the modified Bessel function of zeroth order.

Figures 1(a) and (b) in Sec. 2 show examples of the work PDF (56) for one step, Fig. 1(c) gives an example of the work PDF in Eq. (57) for two positive steps, and in addition further examples are displayed for two and three steps.

#### 4.2. Coefficients of the polynomials

When writing the polynomials as

$$Q_n(\xi) = \sum_{j=0}^n q_j \xi^j, \quad (58)$$

the coefficient  $q_0 = 1$  is fixed by the normalization and the higher-order coefficients  $q_j$ ,  $j = 1, \dots, n$  describe moments of the work  $W_n$ , as discussed in Sec. 2. We now determine all  $q_j$  by starting with Eq. (50) and expressing all matrices  $\mathbb{L}(\xi\epsilon_k)$  as  $\mathbb{I} + \xi\epsilon_k\mathbb{E}_+$ , where  $\mathbb{E}_+ = |0, 1\rangle\langle 1, 0|$ . This generates  $2^n$  products of simpler terms.

The coefficient  $q_1$  is determined by  $n$  terms which contain one matrix  $\mathbb{E}_+$ . Each of these terms factorizes into a product of two elements. The term ending with the ket  $|0, 1\rangle$  is equal to one. The term starting with  $\langle 1, 0|$  is  $r_k$ . Thus the coefficient reads

$$q_1 = \sum_{j=1}^n \epsilon_j r_{j-1}, \quad (59)$$

where the scaled variances  $r_j$  are given in Eq. (34).

The coefficient  $q_2$  is determined by keeping the terms with products of two matrices  $\mathbb{E}_+$ . Defining

$$\phi_{j_2, j_1} = \sum_{j=j_1}^{j_2} \phi_j, \quad (60)$$

for  $0 \leq j_1 < j_2 \leq n$ , the quadratic coefficient can be written as

$$q_2 = \sum_{j_1=1}^{n-1} \epsilon_{j_1} \phi_{j_1-1, 0} \sum_{j_2=j_1+1}^n \epsilon_{j_2} \phi_{j_2-1, j_1}. \quad (61)$$

Continuing this reasoning, one can determine the  $q_j$  for all  $j = 1, \dots, n$ , which are given in Eq. (11). The coefficient  $q_n$  appears in the factorization of  $Q_n(\xi)$ , see also Eq. (16). It is given by the term in Eq. (50) that contains  $n$  matrices  $\mathbb{E}_+$  and can also be written in the simple form

$$q_n = \frac{1}{\phi_n} \prod_{j=1}^n \epsilon_j \phi_j. \quad (62)$$

All coefficients are real and continuous functions of the parameters describing the protocol. Analogously, all coefficients  $p_j$  defining the polynomials  $P_n(\xi) = \sum_{j=0}^n p_j \xi^j$  with  $p_0 = r_n$  can be determined.

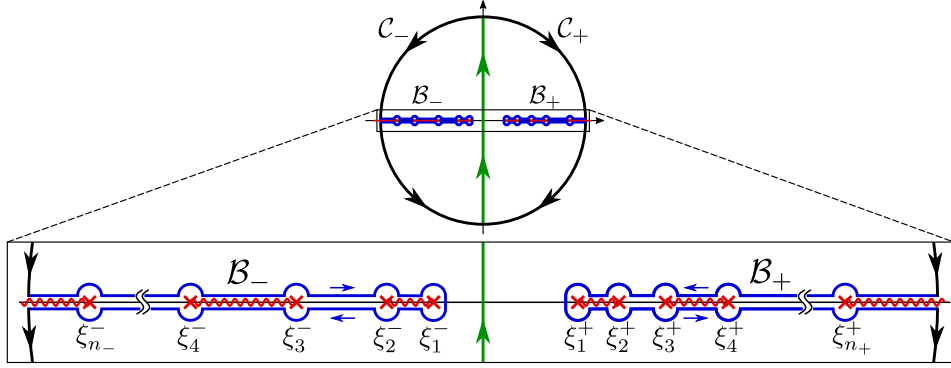


**Figure 3.** Branch cut integration used for the inverse Laplace transform in Eq. (16). The integration path over the imaginary axis is replaced by the path  $\mathcal{B}_-$  for  $w > 0$  (corresponding to closing the contour in the left half plane) and by the path  $\mathcal{B}_+$  for  $w < 0$  (right half plane). It leads to a summation over integrals along branch cuts on the negative (positive) real axis for positive (negative) work values. The branch cuts are indicated by the wavy lines and connect pairs  $(\xi_{2j-1}^\pm, \xi_{2j}^\pm)$  of roots of the polynomial  $Q_n(\xi)$ . If the number  $n_-$  ( $n_+$ ) of negative (positive) roots is odd, an additional integration over the branch cut from  $\xi_{n_-}^-$  ( $\xi_{n_+}^+$ ) to  $-\infty$  ( $+\infty$ ) needs to be taken into account.

#### 4.3. Roots of the polynomials and explicit form of work probability density

To perform the inverse two-sided Laplace transformation of the function (48), the polynomials  $Q_n(\xi)$  are factored as in Eq. (15), which leads to the integral representation (16) of  $\Phi_n(w)$ . One can prove that all roots are real, because otherwise the work distribution obtained from the inverse Laplace transform would exhibit oscillatory behaviour and could become negative.

We now describe the details of the contour integration leading to Eqs. (17)-(22). The roots  $\xi_j^\pm$  become branch points of  $\sqrt{Q_n(\xi)}$ . As illustrated in Fig. 3, we define branch cuts between neighbouring pairs of roots  $\xi_{2j-1}^\pm$  and  $\xi_{2j}^\pm$ ,  $j = 1, \dots, m_\pm$  with  $m_\pm$  given in Eq. (20), and additional branch cuts from  $\xi_{n_\pm}^\pm$  to  $\pm\infty$  if  $n_\pm$  is odd. If  $w > 0$  ( $w < 0$ ), we close the integration path in the left (right) complex half-plane, corresponding to the integration paths  $\mathcal{C}_-$  ( $\mathcal{C}_+$ ) in Fig. 3. This leads to the decomposition (17) into  $\Phi_n^\pm$  for positive and negative work values. The integration over the circular arcs of  $\mathcal{C}_\pm$  vanishes. Each negative (positive) root yields a positive (negative) contribution to the work, i.e. it must correspond to a positive (negative) step of the protocol. Using Cauchy's theorem, we obtain

$$\Phi_n^\pm(w) = -\frac{1}{2\pi i \sqrt{q_n}} \int_{\mathcal{B}_\mp} d\xi \frac{\exp(\beta w \xi)}{\sqrt{\prod_{j=1}^{n_-} (\xi - \xi_j^-) \prod_{k=1}^{n_+} (\xi - \xi_k^+)}} \quad (63)$$

where  $\mathcal{B}_-$  is the path along the negative real axis from  $-\infty$  to  $\xi_1^-$ , which encircles this right-most negative root, and returns below the negative real axis from  $\xi_1^-$  to  $-\infty$  (and analogous for the path  $\mathcal{B}_+$  along the positive real axis).

The contribution of the branch cut between  $\xi_{2j}^-$  and  $\xi_{2j-1}^-$  to the integral (63) is

$$\frac{1}{\pi \sqrt{q_n} i^{n+} (-1)^{j-1}} \int_{\xi_{2j}^-}^{\xi_{2j-1}^-} d\xi \frac{\exp(\beta w \xi)}{\sqrt{\prod_{j=1}^{n_-} |\xi - \xi_j^-| \prod_{k=1}^{n_+} |\xi - \xi_k^+|}}. \quad (64)$$

Analogously, the branch cut between  $\xi_{2j-1}^+$  and  $\xi_{2j}^+$  contributes to the integral (63) by the term

$$\frac{1}{\pi \sqrt{q_n} i^{n+} (-1)^{j-1}} \int_{\xi_{2j-1}^+}^{\xi_{2j}^+} d\xi \frac{\exp(\beta w \xi)}{\sqrt{\prod_{j=1}^{n_-} |\xi - \xi_j^-| \prod_{k=1}^{n_+} |\xi - \xi_k^+|}}. \quad (65)$$

The branch cuts from  $\xi_{n_\pm}^\pm$  to  $\pm\infty$  only contribute if  $n_\pm$  are odd and the integration over them gives

$$\frac{\pm 1}{\pi \sqrt{q_n} i^{n+} (-1)^{m_\pm}} \int_{\xi_{n_\pm}^\pm}^{\pm\infty} d\xi \frac{\exp(\beta w \xi)}{\sqrt{\prod_{j=1}^{n_-} |\xi - \xi_j^-| \prod_{k=1}^{n_+} |\xi - \xi_k^+|}}. \quad (66)$$

Summing up these contributions and considering that  $\sqrt{q_n} = i^{n+} \sqrt{\prod_{j=1}^{n_-} |\xi_j^-| \prod_{k=1}^{n_+} \xi_k^+}$  yields Eqs. (17)-(22).

Some important properties of the polynomials and their roots can be deduced from general properties of the work PDF. The normalization of  $\Phi_n(w)$  is equivalent to  $\tilde{\Phi}_n(u=0) = 1$  and accordingly  $Q_n(0) = 1$ , see Eq. (5). This implies that there is no root at  $\xi = 0$ . We could thus choose the imaginary axis as integration path for the inverse Laplace transform in Eq. (16).

If the last value of the scaled stiffness  $\gamma_n$  is positive, the particle position remains confined by the parabolic potential for all times  $t > t_n$ . This means that the Jarzynski equality [25] can be applied, which is related to the value  $Q_n(1)$ ,

$$\langle e^{-\beta W_n} \rangle = \tilde{\Phi}_n(\beta) = \frac{1}{\sqrt{Q_n(1)}} = \exp \{ -\beta [F_{\text{eq}}(\gamma_n) - F_{\text{eq}}(\gamma_0)] \}, \quad (67)$$

where  $F_{\text{eq}}(\gamma)$  is the free energy of the equilibrium state in the parabolic potential with scaled stiffness  $\gamma$  at temperature  $T = k_B/\beta$ , i.e.  $F_{\text{eq}}(\gamma) = -[1 + \log(2\pi D/\gamma)]/2\beta$ . Inserting this into Eq. (67) gives

$$Q_n(1) = \frac{\gamma_n}{\gamma_0}. \quad (68)$$

One can use the recurrence relation (47) to verify this result. It is valid even for  $\gamma_n \leq 0$  but then the average  $\langle \exp(-\beta W_n) \rangle$  in the Jarzynski equality does not exist. From the general properties of inverse Laplace transform [64] (or from Eq. (65) for  $j = 1$ ) it follows that  $\Phi_n(w) \sim |w|^{-1/2} \exp(\xi_1^+ \beta w)$  for  $w \rightarrow -\infty$ . This implies that the average of  $\exp(-\beta W_n)$  must diverge for  $\xi_1^+ \in ]0, 1]$ . In fact, for  $\xi_1^+ = 1$  the scaled stiffness  $\gamma_n$  must be zero according to Eqs. (15) and (68). A smallest positive root  $\xi_1^+ \in ]0, 1[$  corresponds to a value  $\gamma_n < 0$ . For  $\gamma_n > 0$ , we have no roots in the interval  $[0, 1]$ .

The left panel of Fig. 4 demonstrates the behaviour of  $Q_n(\xi)$  (red lines) for the three-step protocol where the work PDF is shown in Fig. 1(e). In this case with only positive steps all roots are negative. The right panel of Fig. 4 exemplifies the case of a protocol



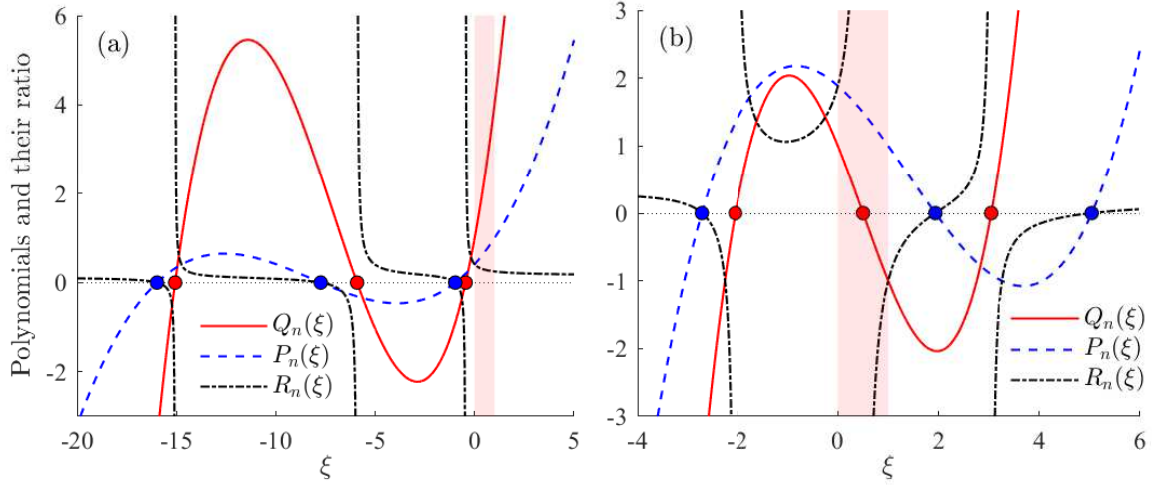


**Figure 4.** Polynomials  $P_3(\xi)$  (blue lines) and  $Q_3(\xi)$  (red lines), together with their ratio  $R_3(\xi)$  (black lines). Circles mark roots of the polynomials. In the left panel, the functions are shown for the protocol with three positive steps:  $\gamma_0 = 1$ ,  $\gamma_1 = 2$ ,  $\gamma_2 = 3$ , and  $\gamma_3 = 4$ ; durations of steps equal to 0.1 (in units of  $1/\gamma_0$ ). All roots of  $Q_3(\xi)$  are negative and hence  $\Phi_3(w)$  is zero for  $w < 0$  as the work PDF in Fig. 1(c) plotted for a similar protocol. In the right panel, the functions are shown for the protocol  $\gamma_0 = 1$ ,  $\gamma_1 = -1$ ,  $\gamma_2 = 1$ , and  $\gamma_3 = -1$ , with step durations 0.1. Since the final value of the protocol is negative, one root occurs in the shaded region with  $\xi \in ]0, 1[$ .

with  $\gamma_n < 0$ , where the particle position has no equilibrium state for long times. In agreement with our general analysis above, the smallest positive root lies in the interval  $]0, 1[$ . For completeness, we also show  $P_n(\xi)$  (blue lines) and  $R_n(\xi) = P_n(\xi)/Q_n(\xi)$  (black lines) in both panels.

The Crooks fluctuation theorem [24] relates the work PDF  $\bar{\Phi}_n(w)$  of the time-reversed protocol  $\bar{\gamma}(t)$  where  $\bar{\gamma}_j = \gamma_{n-j}$  (and durations of segments being the same) to  $\Phi_n(w)$  as

$$\bar{\Phi}_n(w) = \Phi_n(-w) \exp \{ \beta [w + F_{\text{eq}}(\gamma_n) - F_{\text{eq}}(\gamma_0)] \}. \quad (69)$$

It implies the following relation between the polynomials  $\bar{Q}_n(\xi)$  and  $Q_n(\xi)$  for the reversed and original protocol:

$$\bar{Q}_n(\xi) = \frac{\gamma_0}{\gamma_n} Q_n(1 - \xi). \quad (70)$$

This relation can, for example, be used to check implementations of the numerical scheme discussed in Sec. 2.

## 5. Summary and perspectives

In summary, we studied the driven Brownian particle in a time-dependent parabolic potential and heat bath environment at temperature  $T$ . Initially the particle position is equilibrated and a piecewise constant time-evolution of the stiffness of the potential is considered. We derived an exact analytical result for the joint distribution of the work

done on the particle and its position for a general protocol with  $n$  steps. It is determined by a rational function that satisfies a recurrence relation, whose explicit solution is a finite regular continued fraction. Rewriting the continued fraction as ratio  $P_n/Q_n$  of two polynomials  $P_n$  and  $Q_n$  of order  $n$ , we showed that  $1/\sqrt{Q_n}$  gives the moment generating function of the work. The  $Q_n$  were shown to satisfy a simple recurrence relation and roots of  $Q_n$  have the following properties: (i) all roots are real and to each positive/negative step of the protocol (increasing/decreasing stiffness) corresponds one negative/positive root, (ii) the normalization condition of the work PDF requires that there is no root at zero, (iii) if the final state of the potential has positive stiffness, the Jarzynski equality holds and requires that no root lies in the interval  $[0, 1]$ . With all these properties, one can very efficiently determine the work PDF for even large number  $n$  of steps and thereby obtain excellent approximations for arbitrary continuous-time protocols by a suitable discretization.

From a general perspective, our results are interesting with respect to the problem of finding closed analytical formulas for a larger number of convolutions of Gaussian functions with differing parameters. This problem is important for many fields due to the ubiquitous occurrence of Gaussian processes and related quadratic approximations. In this respect it would be interesting to generalize our methodology to an arbitrary initial condition for the particle position and to a protocol, where in addition to the stiffness the position (minimum) of the parabolic potential is varying in time. From a physical perspective such generalizations may seem to be easily tractable. However, the mathematics requires a nontrivial extension of the methodology as it involves a more complex mapping between the parameters specifying the Gaussian functions. This could lead to further results for recursively defined sequences of polynomials and their relation to structured matrices, continued fractions, moment problems, and root localization [65]. We believe that the physical treatment of corresponding problems will give valuable insight or even solutions for the mathematical convolution problem.

## Acknowledgments

Financial support by the Czech Science Foundation (Project No. 20-24748J) and the Deutsche Forschungsgemeinschaft (Project No. 397157593) is gratefully acknowledged. We sincerely thank the members of the DFG Research Unit FOR 2692 for fruitful discussions. VH also thanks for support by the Humboldt foundation.

## References

- [1] Sekimoto, K. Langevin equation and thermodynamics. *Prog. Theor. Phys. Suppl.* **130**, 17 (1998).
- [2] Seifert, U. Entropy production along a stochastic trajectory and an integral fluctuation theorem. *Phys. Rev. Lett.* **95**, 040602 (2005).
- [3] Ritort, F. Nonequilibrium fluctuations in small systems: From physics to biology. *Adv. Chem. Phys.* **137**, 31 (2008).

- [4] Esposito, M., Harbola, U. & Mukamel, S. Nonequilibrium fluctuations, fluctuation theorems, and counting statistics in quantum systems. *Rev. Mod. Phys.* **81**, 1665 (2009).
- [5] Seifert, U. Stochastic thermodynamics, fluctuation theorems and molecular machines. *Rep. Prog. Phys.* **75**, 126001 (2012).
- [6] Crooks, G. E. Path-ensemble averages in systems driven far from equilibrium. *Phys. Rev. E* **61**, 2361 (2000).
- [7] Jarzynski, C. Nonequilibrium work relations: Foundations and applications. *Eur. Phys. J. B* **64**, 331 (2008).
- [8] Harris, R. J. & Schütz, G. M. Fluctuation theorems for stochastic dynamics. *J. Stat. Mech.* **2007**, P07020 (2007).
- [9] Esposito, M. & Van den Broeck, C. Three faces of the second law. I. Master equation formulation. *Phys. Rev. E* **82**, 011143 (2010).
- [10] Van den Broeck, C. & Esposito, M. Three faces of the second law. II. Fokker-Planck formulation. *Phys. Rev. E* **82**, 011144 (2010).
- [11] Jarzynski, C. Equalities and inequalities: Irreversibility and the second law of thermodynamics at the nanoscale. *Ann. Rev. Cond. Matt. Phys.* **2**, 329 (2011).
- [12] Bochkov, G. N. & Kuzovlev, Y. E. Fluctuation–dissipation relations. Achievements and misunderstandings. *Phys.-Uspekhi* **56**, 590 (2013).
- [13] Maillet, O. *et al.* Optimal probabilistic work extraction beyond the free energy difference with a single-electron device. *Phys. Rev. Lett.* **122**, 150604 (2019).
- [14] Hummer, G. Fast-growth thermodynamic integration: Results for sodium ion hydration. *Mol. Sim.* **28**, 81 (2002).
- [15] Shirts, M. R., Bair, E., Hooker, G. & Pande, V. S. Equilibrium free energies from nonequilibrium measurements using maximum-likelihood methods. *Phys. Rev. Lett.* **91**, 140601 (2003).
- [16] Collin, D. *et al.* Verification of the Crooks fluctuation theorem and recovery of RNA folding free energies. *Nature* **437**, 231 (2005).
- [17] Pohorille, A., Jarzynski, C. & Chipot, C. Good practices in free-energy calculations. *J. Phys. Chem. B* **114**, 10235 (2010).
- [18] Kim, S., Kim, Y. W., Talkner, P. & Yi, J. Comparison of free-energy estimators and their dependence on dissipated work. *Phys. Rev. E* **86**, 041130 (2012).
- [19] Dellago, C. & Hummer, G. Computing equilibrium free energies using non-equilibrium molecular dynamics. *Entropy* **16**, 41 (2014).
- [20] Ribezzi-Crivellari, M. & Ritort, F. Free-energy inference from partial work measurements in small systems. *Proc. Natl. Acad. Sci. U.S.A.* **111**, E3386 (2014).
- [21] Yunger Halpern, N. & Jarzynski, C. Number of trials required to estimate a free-energy difference, using fluctuation relations. *Phys. Rev. E* **93**, 052144 (2016).
- [22] Arrar, M. *et al.* On the accurate estimation of free energies using the Jarzynski equality. *J. Comput. Chem.* **40**, 688 (2019).
- [23] Crooks, G. E. Nonequilibrium measurements of free energy differences for microscopically reversible Markovian systems. *J. Stat. Phys.* **90**, 1481 (1998).
- [24] Crooks, G. E. Entropy production fluctuation theorem and the nonequilibrium work relation for free energy differences. *Phys. Rev. E* **60**, 2721 (1999).
- [25] Jarzynski, C. Nonequilibrium equality for free energy differences. *Phys. Rev. Lett.* **78**, 2690 (1997).
- [26] Jarzynski, C. Equilibrium free-energy differences from nonequilibrium measurements: A master-equation approach. *Phys. Rev. E* **56**, 5018 (1997).
- [27] Severino, A., Monge, A. M., Rissone, P. & Ritort, F. Efficient methods for determining folding free energies in single-molecule pulling experiments. *J. Stat. Mech.* **2019**, 124001 (2019).
- [28] Palassini, M. & Ritort, F. Improving free-energy estimates from unidirectional work measurements: Theory and experiment. *Phys. Rev. Lett.* **107**, 060601 (2011).
- [29] Holubec, V., Lips, D., Ryabov, A., Chvosta, P. & Maass, P. On asymptotic behavior of work

- distributions for driven Brownian motion. *Eur. Phys. J. B* **88**, 340 (2015).
- [30] Trepagnier, E. H. *et al.* Experimental test of Hatano and Sasa's nonequilibrium steady-state equality. *Proc. Natl. Acad. Sci. U.S.A.* **101**, 15038 (2004).
  - [31] Carberry, D. M. *et al.* Fluctuations and irreversibility: An experimental demonstration of a second-law-like theorem using a colloidal particle held in an optical trap. *Phys. Rev. Lett.* **92**, 140601 (2004).
  - [32] Carberry, D. M., Baker, M. A. B., Wang, G. M., Sevick, E. M. & Evans, D. J. An optical trap experiment to demonstrate fluctuation theorems in viscoelastic media. *J. Optics A* **9**, S204 (2007).
  - [33] Andrieux, D. *et al.* Entropy production and time asymmetry in nonequilibrium fluctuations. *Phys. Rev. Lett.* **98**, 150601 (2007).
  - [34] Khan, M. & Sood, A. K. Irreversibility-to-reversibility crossover in transient response of an optically trapped particle. *EPL* **94**, 60003 (2011).
  - [35] Mestres, P., Martinez, I. A., Ortiz-Ambriz, A., Rica, R. A. & Roldan, E. Realization of nonequilibrium thermodynamic processes using external colored noise. *Phys. Rev. E* **90**, 032116 (2014).
  - [36] Engel, A. Asymptotics of work distributions in nonequilibrium systems. *Phys. Rev. E* **80**, 021120 (2009).
  - [37] Nickelsen, D. & Engel, A. Asymptotics of work distributions: The pre-exponential factor. *Eur. Phys. J. B* **82**, 207 (2011).
  - [38] Noh, J. D., Kwon, C. & Park, H. Multiple dynamic transitions in nonequilibrium work fluctuations. *Phys. Rev. Lett.* **111**, 130601 (2013).
  - [39] Ryabov, A., Dierl, M., Chvosta, P., Einax, M. & Maass, P. Work distribution in a time-dependent logarithmic-harmonic potential: Exact results and asymptotic analysis. *J. Phys. A* **46**, 075002 (2013).
  - [40] Manikandan, S. K. & Krishnamurthy, S. Asymptotics of work distributions in a stochastically driven system. *Eur. Phys. J. B* **90**, 258 (2017).
  - [41] van Zon, R. & Cohen, E. G. D. Stationary and transient work-fluctuation theorems for a dragged Brownian particle. *Phys. Rev. E* **67**, 046102 (2003).
  - [42] van Zon, R. & Cohen, E. G. D. Extended heat-fluctuation theorems for a system with deterministic and stochastic forces. *Phys. Rev. E* **69**, 056121 (2004).
  - [43] Cohen, E. G. D. Properties of nonequilibrium steady states: A path integral approach. *J. Stat. Mech.* **2008**, P07014 (2008).
  - [44] Subaşı, Y. & Jarzynski, C. Microcanonical work and fluctuation relations for an open system: An exactly solvable model. *Phys. Rev. E* **88**, 042136 (2013).
  - [45] Kim, K., Kwon, C. & Park, H. Heat fluctuations and initial ensembles. *Phys. Rev. E* **90**, 032117 (2014).
  - [46] Speck, T. Work distribution for the driven harmonic oscillator with time-dependent strength: Exact solution and slow driving. *J. Phys. A* **44**, 305001 (2011).
  - [47] Kwon, C., Noh, J. D. & Park, H. Nonequilibrium fluctuations for linear diffusion dynamics. *Phys. Rev. E* **83**, 061145 (2011).
  - [48] Kwon, C., Noh, J. D. & Park, H. Work fluctuations in a time-dependent harmonic potential: Rigorous results beyond the overdamped limit. *Phys. Rev. E* **88**, 062102 (2013).
  - [49] Hoppenau, J. & Engel, A. On the work distribution in quasi-static processes. *J. Stat. Mech.* **2013**, P06004 (2013).
  - [50] Deza, R. R., Izús, G. G. & Wio, H. S. Fluctuation theorems from non-equilibrium Onsager-Machlup theory for a Brownian particle in a time-dependent harmonic potential. *Centr. Eur. J. Phys.* **7**, 472 (2009).
  - [51] Holubec, V., Kroy, K. & Steffenoni, S. Physically consistent numerical solver for time-dependent Fokker-Planck equations. *Phys. Rev. E* **99**, 032117 (2019).
  - [52] Imparato, A. & Peliti, L. Work probability distribution in single-molecule experiments. *EPL* **69**,

- 643 (2005).
- [53] Šubr, E. & Chvosta, P. Exact analysis of work fluctuations in two-level systems. *J. Stat. Mech.* **2007**, P09019 (2007).
  - [54] Chvosta, P. & Reineker, P. Dynamics under the influence of semi-Markov noise. *Physica A* **268**, 103 (1999).
  - [55] Proesmans, K., Driesen, C., Cleuren, B. & Van den Broeck, C. Efficiency of single-particle engines. *Phys. Rev. E* **92**, 032105 (2015).
  - [56] Proesmans, K., Cleuren, B. & den Broeck, C. V. Linear stochastic thermodynamics for periodically driven systems. *J. Stat. Mech.* **2016**, 023202 (2016).
  - [57] Holubec, V. & Ryabov, A. Work and power fluctuations in a critical heat engine. *Phys. Rev. E* **96**, 030102 (2017).
  - [58] Pietzonka, P. & Seifert, U. Universal trade-off between power, efficiency, and constancy in steady-state heat engines. *Phys. Rev. Lett.* **120**, 190602 (2018).
  - [59] Holubec, V. & Ryabov, A. Cycling tames power fluctuations near optimum efficiency. *Phys. Rev. Lett.* **121**, 120601 (2018).
  - [60] Solon, A. P. & Horowitz, J. M. Phase transition in protocols minimizing work fluctuations. *Phys. Rev. Lett.* **120**, 180605 (2018).
  - [61] Brown, A. I. & Sivak, D. A. Theory of nonequilibrium free energy transduction by molecular machines. *Chem. Rev.* **120**, 434 (2020).
  - [62] Grebenkov, D. S. Probability distribution of the time-averaged mean-square displacement of a Gaussian process. *Phys. Rev. E* **84**, 031124 (2011).
  - [63] Andrianov, A. & Grebenkov, D. S. Time-averaged MSD of Brownian motion. *J. Stat. Mech.* **2012**, P07001 (2012).
  - [64] Doetsch, G. *Introduction to the Theory and Application of the Laplace Transformation* (Springer, 1974). Chapter 37 on Page 250.
  - [65] Holtz, O. & Tyaglov, M. Structured matrices, continued fractions, and root localization of polynomials. *SIAM Review* **54**, 421 (2012).